NUCLEAR THEORY, Vol. 42 (2025)
eds. M. Gaidarov, N. Minkov, Heron Press, Sofia

Short-Range Correlations and Meson-Exchage Currents in Electron and Neutrino Scattering

P.R. Casale [1,2], **J.E. Amaro**[1,2]

[1]Departamento de Fisica Atomica, Molecular y Nuclear,
Universidad de Granada, 18071 Granada, Spain
[2]Instituto Carlos I de Fisica Teorica y Computacional,
Universidad de Granada, 18071 Granada, Spain

Abstract. We investigate meson-exchange currents (MEC) in the one-particle emission transverse response of nuclear matter, incorporating short-range correlations via the Bethe-Goldstone equation with a realistic nucleon-nucleon interaction. The interference between one-body and two-body currents, strengthened by the high-momentum components of correlated pairs, produces a marked enhancement of the transverse response. We also indicate how the formalism extends to neutrino scattering, where similar effects are expected to impact oscillation experiments.

1 Introduction

There is clear experimental evidence of an enhancement of the transverse response in the quasielastic peak with respect to single-particle models in the 1p1h channel [1,2]. Two-particletwo-hole (2p2h) excitations induced by meson-exchange currents (MEC) are not sufficient to explain this effect, since their main contribution lies in the dip region between quasielastic and pion production [3]. Ab initio calculations in light nuclei also find a transverse enhancement produced by MEC, although they cannot disentangle between 1p1h and 2p2h channels [4, 5]. For heavier nuclei and nuclear matter, however, single-particle models consistently predict that MEC reduce the 1p1h transverse response, mainly due to the Δ current [6–10], a result corroborated in recent comparisons across different single-particle approaches, including the spectral function model [11]. In contrast, the calculation of Fabrocini within the correlated basis function (CBF) framework found an enhancement in nuclear matter due to the combined effect of short-range correlations (SRC) and MEC [12].

Motivated by this, in the present work we develop a correlated model of the transverse response in the 1p1h channel that includes MEC within the independent pair approximation. This is made possible by our recent solution of the Bethe-Goldstone equation for two correlated nucleons in nuclear matter, which provides wave functions with explicit high-momentum components [13]. Here we apply this framework to investigate whether correlations together with MEC are sufficient to account for the observed transverse enhancement.

2 Analysis of SRC Using the Bethe-Goldstone Equation

In order to describe short-range correlations (SRC) in nuclear matter we solve the Bethe-Goldstone (BG) equation for a correlated pair of nucleons [14, 15]. We assume that two nucleons interact in the presence of a degenerate Fermi gas. The Pauli exclusion principle forbids them from scattering into already occupied states, and as a consequence their wave function is modified by the interaction and acquires high-momentum components above the Fermi surface,

$$\Psi = \Psi_0 + Q\Psi, \tag{1}$$

where Q is the Pauli blocking projector over high momenta $> k_F$,

$$Q|p_1' p_2'\rangle = \begin{cases} |p_1' p_2'\rangle & \text{if} \quad |p_i'| > k_F, \\ 0 & \text{otherwise.} \end{cases} \tag{2}$$

We assume that the uncorrelated and correlated wave functions satisfy the two-body Schrodinger equation with the same energy

$$T\Psi_0 = E\Psi_0, \qquad (T+V)\Psi = E\Psi, \tag{3}$$

where V is the NN potential. Operating with $(E-T)$ and solving for $Q\Psi$, one obtains the BG equation for a correlated pair,

$$\Psi = \Psi_0 + \frac{Q}{E-T} V\Psi. \tag{4}$$

Expressed in integral form, the BG equation reads

$$|\Psi\rangle = |\mathbf{P},\mathbf{p}\rangle + \int d^3\mathbf{P}' d^3\mathbf{p}' \frac{Q(\mathbf{P}',\mathbf{p}')}{\frac{(\mathbf{P}^2-\mathbf{P}'^2)}{2M_T} - \frac{(\mathbf{p}^2-\mathbf{p}'^2)}{2\mu}} |\mathbf{P}',\mathbf{p}'\rangle\langle\mathbf{P}',\mathbf{p}'|V|\Psi\rangle.$$

where $\mathbf{P} = \mathbf{p}_1 + \mathbf{p}_2$ is the total momentum of two nucleons in the Fermi gas, below the Fermi momentum, $p_1, p_2 < k_F$, and $\mathbf{p} = (\mathbf{p}_1 - \mathbf{p}_2)/2$ is the relative momentum. Since the nucleon-nucleon potential depends only on the relative coordinate $\mathbf{r} = \mathbf{r}_1 - \mathbf{r}_2$,

$$\langle\mathbf{P}',\mathbf{p}'|V|\Psi\rangle = \delta(\mathbf{P}'-\mathbf{P})\,\langle\mathbf{p}'|V|\psi\rangle, \tag{5}$$

where $\psi(\mathbf{r})$ is the relative wave function of the nucleon pair, verying the integral BG equation

$$|\psi\rangle = |\mathbf{p}\rangle + \int d^3\mathbf{p}'\, \frac{Q(\mathbf{P},\mathbf{p}')}{p^2-p'^2} |\mathbf{p}'\rangle\langle\mathbf{p}'|2\mu V|\Psi\rangle. \tag{6}$$

This equation is further simplified by performing an angular average of the Pauli blocking operator Q, so that it depends only on the moduli of the center-of-mass momentum P and the relative momentum p [13]. This simplification is convenient for performing the multipole expansion of the wave function.

The correlated relative wave function is a bispinor, reflecting the fact that the nucleons are spin-$\frac{1}{2}$ particles. Since the nucleon-nucleon potential does not mix spin channels, we can treat separately the cases singlet ($S = 0$) and triplet ($S = 1$) and perform a multipole expansion,

$$|\psi\rangle = |\mathbf{p}, SM_s\rangle + |\Delta\psi\rangle, \tag{7}$$

$$\langle \mathbf{r}|\mathbf{p}, S, M_s\rangle = \sqrt{\frac{2}{\pi}} \sum_{JM} \sum_{lm_l} i^l Y^*_{lm_l}(\hat{\mathbf{p}}) \langle lm_l SM_s|JM\rangle j_l(pr)\, \mathcal{Y}_{lSJM}(\hat{\mathbf{r}}), \tag{8}$$

$$\langle \mathbf{r}|\Delta\psi\rangle = \sqrt{\frac{2}{\pi}} \sum_{JM} \sum_{ll'm_l} i^{l'} Y^*_{l'm_l}(\hat{\mathbf{p}}) \langle l'm_l SM_s|JM\rangle \Delta\phi^{SJ}_{ll'}(r)\, \mathcal{Y}_{lSJM}(\hat{\mathbf{r}}), \tag{9}$$

where

$$\mathcal{Y}_{lSJM}(\hat{\mathbf{r}}) = \sum_{m\mu} \langle lmS\mu|JM\rangle\, Y_{lm}(\hat{\mathbf{r}})\, |S\mu\rangle, \tag{10}$$

The functions $\Delta\phi^{SJ}_{ll'}(r)$ represent the high-momentum components of the radial part of the correlated wave function. By substituting the partial-wave expansion into the integral BG equation, one obtains a set of coupled equations for each spin-total angular momentum channel SJ,

$$u^{SJ}_{ll'}(r) = \delta_{ll'} \hat{j}_l(pr) + \int dr'\, \hat{G}_l(r, r') \sum_{l_1} U^{SJ}_{l_1 l}(r')\, u^{SJ}_{l_1 l'}(r'). \tag{11}$$

Here, $u^{SJ}_{ll'}(r)$ are the reduced radial wave functions, defined as the full radial wave functions multiplied by r, while $\hat{j}_l(pr)$ are the reduced spherical Bessel functions. The kernel $\hat{G}_l(r, r')$ is the reduced Green function of the equation, which can be found in detail in Ref. [13]. The functions $U^{SJ}_{l_1 l}(r)$ are the multipoles of the nucleon-nucleon potential in the S, J channel, multiplied by the nucleon mass.

Table 1 summarizes the partial-wave decomposition of the correlated two-nucleon system, listing the total spin S, total angular momentum J, orbital angular momenta (l, l'), and the corresponding channels, including coupled and uncoupled cases where tensor mixing occurs.

Table 1. Partial-wave decomposition of the correlated two-nucleon system

S	J	(l, l')	Channels
0	$l = l'$	any	${}^1S_0, {}^1P_1, {}^1D_2, {}^1F_3$
1	0	$l = l' = 1$	${}^3P_0$
1	≥ 1 uncoupled	$l = l' = J$	${}^3P_1, {}^3D_2, \ldots$
1	1 coupled	(0,2)	${}^3S_1, {}^3D_1$ with mixing ${}^3S_1/{}^3D_1$
1	2 coupled	(1,3)	${}^3P_2, {}^3F_2$ with mixing ${}^3P_2/{}^3F_2$
1	3 coupled	(2,4)	${}^3D_3$

2.1 Solution of the BG equation with a delta-shell potential

We solve the BG equation for the Granada 2013 potential [16],

$$U_{ll'}^{SJ}(r) = \sum_{i=1}^{N} (\lambda_i)_{ll'}^{SJ}\, \delta(r - r_i), \tag{12}$$

where there are $N = 5$ delta shells at positions r_i and strengths $(\lambda_i)_{ll'}^{SJ}$. The potential was obtained through a partial wave analysis of np and pp scattering data below the pion production threshold. Its coarse-grained form reflects the fact that the nucleon wavelength cannot resolve details of the interaction at distances smaller than $\Delta r \sim 0.6$ fm. In this case the radial BG equation becomes

$$u_{ll'}^{SJ}(r) = \hat{j}_l(pr)\delta_{ll'} + \sum_i \hat{G}_l(r, r_i) \sum_{l_1} (\lambda_i)_{l_1 l}^{SJ}\, u_{l_1 l'}^{SJ}(r_i). \tag{13}$$

Taking $r = r_j$ leads to a closed linear system for $u_{ll'}^{SJ}(r_j)$, which is solved separately for uncoupled and coupled partial waves,

$$u_{ll'}^{SJ}(r_j) \;=\; \hat{j}_l(pr_j)\,\delta_{ll'} + \sum_i \hat{G}_l(r_j, r_i) \sum_{l_1} (\lambda_i)_{l_1 l}^{SJ}\, u_{l_1 l'}^{SJ}(r_i), \tag{14}$$

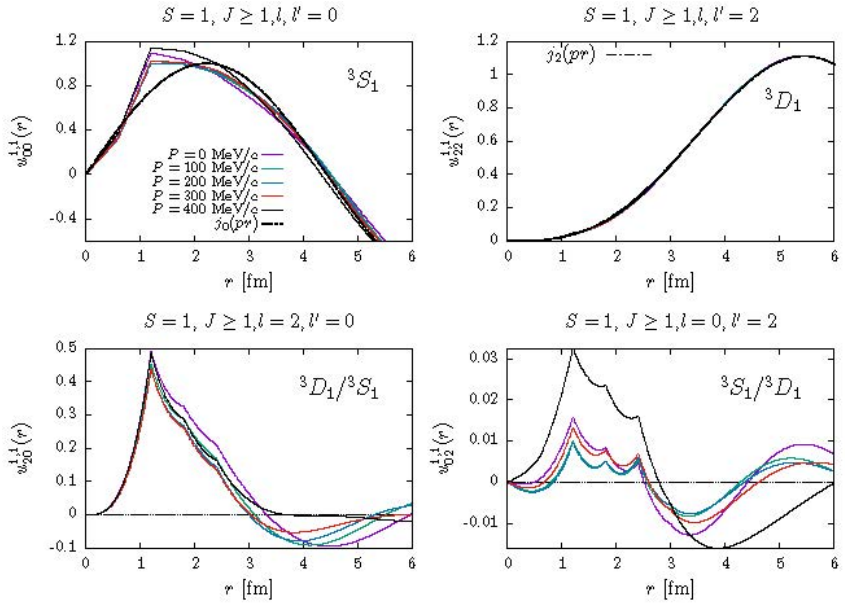

Figure 1. Example of coupled radial wave functions $u_{ll'}^{SJ}(r)$ obtained from the Bethe–Goldstone equation. The relative momentum of the pair is $p = 225$ MeV/c. We see the results for several values of the total momentum P.

where r_j are the discretized mesh points, The uncoupled channels lead to a system of 5 linear equations, which can be solved trivially by matrix inversion, essentially in analytical form. The coupled channels correspond to two linear systems of 10 equations each, which are solved in an equally straightforward manner.

In Figure 1 we show an example of the solutions for the coupled $J = 1$ channel. The solutions correspond to the linear system for $(l = 0, 2;\ l' = 0)$ and another for $(l = 0, 2;\ l' = 2)$. The most important contribution arises from the $(l, l' = 0, 2;\ l' = 0)$ case. In particular, we observe a strong mixing between the ${}^3S_1$ and ${}^3D_1$ waves, showing that this coupled channel is especially important. The mixing is driven by the tensor component of the nucleon–nucleon interaction, which generates high-momentum components in the correlated two-body wave function. These components are crucial for describing short-range correlations and directly affect the interference between one- and two-body currents in the transverse response.

The solution of the BG equation can also be expressed in momentum space, leading to correlated partial waves $\phi_{ll'}^{SJ}(p')$ that exhibit the high-momentum tails induced by SRC. These functions are obtained directly as the Fourier transform of the coordinate-space solutions $u_{ll'}^{SJ}(r)$. We can separate the momentum-space

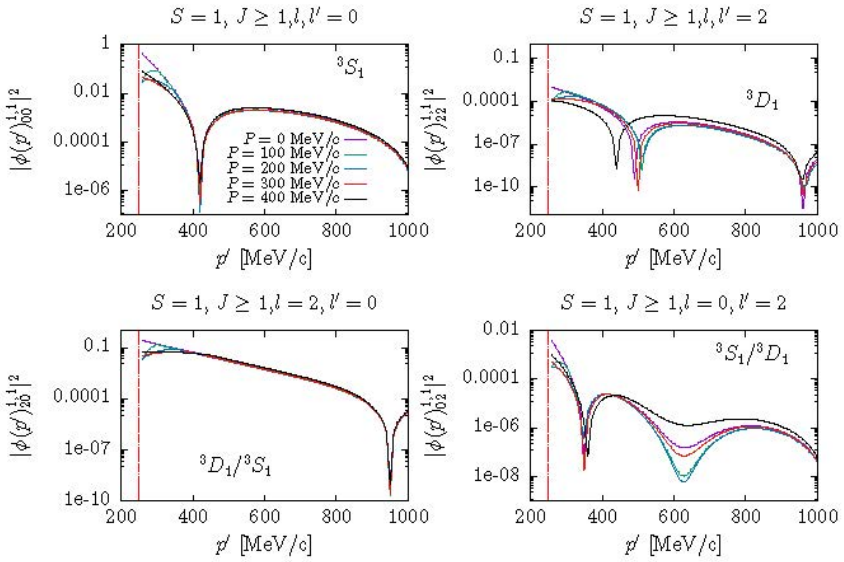

Figure 2. Example of momentum-space correlated wave functions $|\tilde{\Phi}_{ll'}^{SJ}(p')|^2$ in a coupled channel. The emergence of high-momentum components reflects the action of short-range correlations.

solution into a free part and a high momentum component

$$\phi^{SJ}_{ll'}(p') \;=\; \sqrt{\frac{\pi}{2}}\,\frac{1}{pp'}\,\delta(p-p')\,\delta_{ll'} + \Delta\phi^{SJ}_{ll'}(p'), \tag{15}$$

where the high-momentum component is given by

$$\Delta\phi^{SJ}_{ll'}(p') \;=\; \sqrt{\frac{2}{\pi}}\,\frac{1}{pp'}\,\frac{Q(P,p')}{p^2-p'^2}\sum_i \hat{j}_l(p'r_i)\sum_{l_1}(\lambda_i)^{SJ}_{l_1 l}\,u^{SJ}_{l_1 l'}(r_i). \tag{16}$$

In Figure 2 we show an example of the squared amplitude (momentum distribution) of the high-momentum partial waves $\phi^{11}_{ll'}(p')$ for the coupled $S=J=1$ channel of a nucleon pair with relative momentum $p = 225$ MeV/c, evaluated for several values of the total momentum. The largest contributions arise from the $(l,l') = (0,0)\ {}^3S_1$ component and from the $(l,l') = (2,0)\ {}^3S_1$–${}^3D_1$ interference. This dominance reflects the strong tensor mixing in the coupled ${}^3S_1{}^3D_1$ channel, which generates the leading high-momentum components of the wave function.

3 SRC and MEC in QE Electron Scattering

In QE electron scattering the longitudinal and transverse responses correspond to $R_L(q,\omega) = W^{00}$ and $R_T(q,\omega) = W^{11} + W^{22}$, respectively, where the hadronic tensor in the RFG model is given by

$$W^{\mu\mu} = \sum_{ph} |\langle ph^{-1}|J^\mu(\mathbf{q})|F\rangle|^2\theta(p-k_F)\theta(k_F-h)\delta(E_p-E_h-\omega),$$

Here we consider the non-relativistic current operator, written as the sum of one-body and two-body meson-exchange current (MEC) contributions at leading order, $\mathbf{J} = \mathbf{J}_{1b} + \mathbf{J}_{2b}$. The two-body operator [17, 18] is the sum of the well-known pion-exchange diagrams seagull, pionic or pion-in-flight and Δ currents of Figure 3.

The $1p$–$1h$ matrix element of the current in the Fermi gas can be written as

$$\langle ph^{-1}|J^\mu(\mathbf{q})|F\rangle = \langle p|J^\mu_{1b}(\mathbf{q})|h\rangle + \sum_{k-k_F}\langle pk|J^\mu_{2b}(\mathbf{q})|hk-kh\rangle. \tag{17}$$

Taking the modulus squared, one obtains

$$\begin{aligned}|\langle ph^{-1}|J^\mu(\mathbf{q})|F\rangle|^2 = {}& |\langle p|J^\mu_{1b}(\mathbf{q})|h\rangle|^2 \\ & + 2\,\mathrm{Re}\left[\langle p|J^\mu_{1b}(\mathbf{q})|h\rangle^*\sum_k\langle pk|J^\mu_{2b}(\mathbf{q})|hk-kh\rangle\right] \\ & + \text{ pure two-body MEC terms.}\end{aligned} \tag{18}$$

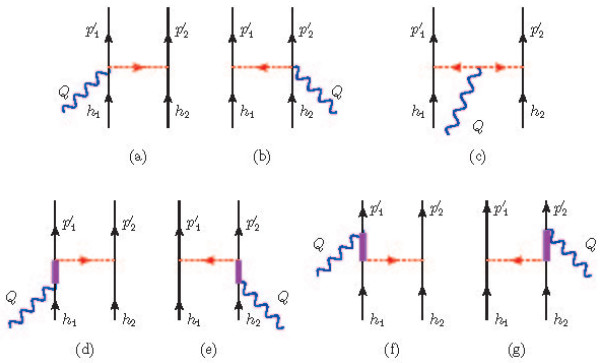

Figure 3. Meson exchange currents contributing to the QE response: seagull, pion-in-flight, and Δ excitation diagrams.

The first term represents the pure one-body contribution, the second term the interference between one- and two-body currents, and the last term the pure MEC contribution, which is typically small and can be neglected to first approximation. Thus the transverse response function can be written schematically as

$$R^T_{FG}(q,\omega) = R^T_{1b}(q,\omega) + R^T_{1b2b}(q,\omega) + \ldots \tag{19}$$

In the Fermi gas, the interference term R^T_{1b2b} is negative due to the partial cancellation between seagull, pion-in-flight, and Δ currents, with the *negative* Δ contribution dominating at intermediate momentum transfers [11].

When short-range correlations (SRC) are included within the independent-pair approximation, the two-body matrix elements must be evaluated with correlated two-particle states, $|\Phi_{hk}\rangle = |hk\rangle + |\Delta\Phi_{hk}\rangle$, rather than the uncorrelated states $|hk\rangle$. Accordingly, the matrix element of the two-body current becomes

$$\begin{aligned}\langle ph^{-1}|J^\mu_{2b}(\mathbf{q})|F\rangle &= \sum_k \langle pk|J^\mu_{2b}(\mathbf{q})|\Phi_{hk} - \Phi_{kh}\rangle \\ &= \sum_k \langle pk|J^\mu_{2b}(\mathbf{q})|hk - kh\rangle + \sum_k \langle pk|J^\mu_{2b}(\mathbf{q})|\Delta\Phi_{hk} - \Delta\Phi_{kh}\rangle. \end{aligned} \tag{20}$$

Thus, in the interference term between one- and two-body currents, a new contribution appears in which the MEC operator acts directly on the high-momentum components of correlated pairs:

$$2\,\mathrm{Re}\left[\langle p|J^\mu_{1b}|h\rangle^* \sum_{k<k_F} \langle pk|J^\mu_{2b}|\Delta\Phi_{hk} - \Delta\Phi_{kh}\rangle\right]. \tag{21}$$

This new correlated MEC contribution can be represented schematically by the diagram of Figure 4, where the two-body operator couples to the high-momentum components (p_1, p_2) of the (hk) pair.

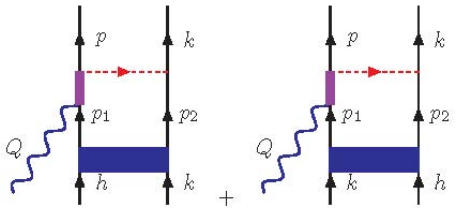

Figure 4. High-momentum MEC contributions induced by SRC in the two-body current.

The transverse response function can then be expressed as the sum of the uncorrelated Fermi gas result (including MEC) plus an additional term driven by SRC:

$$R^T(q,\omega) = R^T_{FG}(q,\omega) + \Delta R^T_{\mathrm{SRC,MEC}}(q,\omega), \tag{22}$$

where $\Delta R^K_{\mathrm{SRC,MEC}}$ originates from the interference between the one-body current and the MEC acting on the high-momentum componets of correlated pairs. This contribution is essential to account for the observed enhancement of the transverse response.

4 Results

In order to compare our calculation with experimental data, it is well known that the simple Fermi gas model is inadequate. Therefore, we adopt a superscaling approach [19], in which the longitudinal scaling function $f_L(\psi')$ is extracted from inclusive electron scattering data on ^{12}C at momentum transfers up to $q \approx 570$ MeV/c [13]. Figure 5 shows the extracted scaling function and the fit used in the present study. The corresponding longitudinal response R_L is well reproduced by this fit, as shown in Figure 6.

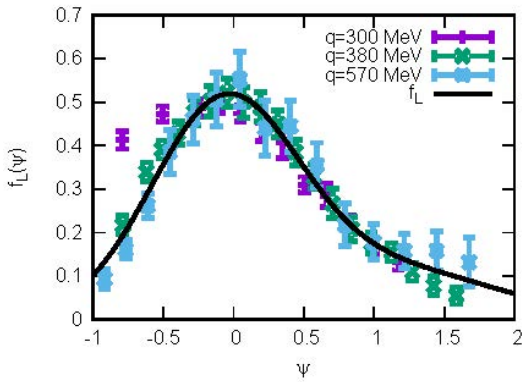

Figure 5. Scaling function $f_L(\psi')$ extracted from ^{12}C data and the SuSA fit.

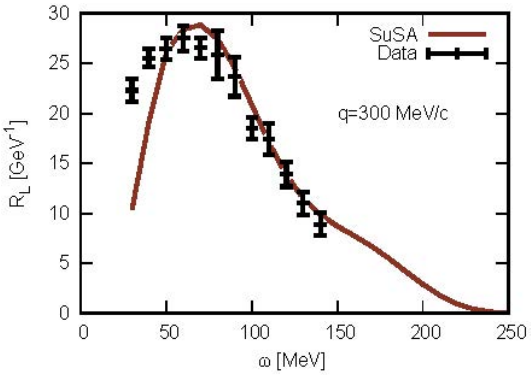

Figure 6. Longitudinal response R_L obtained using the SuSA scaling function. The data are well reproduced.

Assuming scaling of the zero kind, $f_T = f_L$, we investigate the transverse response. Figure 7 shows that the naive Fermi gas calculation with MEC produces a reduction of the transverse response, failing to reproduce the data. By contrast, the inclusion of short-range correlations in the MEC matrix elements, following our independent pair approximation and the Bethe–Goldstone solution, generates an enhancement that cancels the reduction from the FG MEC and successfully reproduces the experimental transverse response.

The enhancement is mainly produced by the interference of the coupled ${}^3S_1$-${}^3D_1$ partial waves, highlighting the crucial role of the tensor force in the correlated wave function. Remarkably, this effect emerges directly from the NN

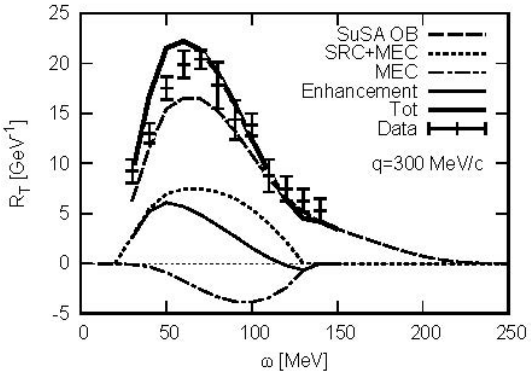

Figure 7. Transverse response R_T showing separate contributions: OB only, OB+MEC in the Fermi gas, and OB+MEC including SRC (high-momentum components). The enhancement arises from the interference of the coupled ${}^3S_1$-${}^3D_1$ channels, i.e., the tensor force.

potential (Granada 2013), fitted to NN cross section data, without any additional parameter or fit for the enhancement. This result aligns with Fabrocini's correlated basis function (CBF) calculations in nuclear matter, showing that despite the different approaches to SRC, both methods produce a similar tendency towards transverse enhancement. Our calculation therefore provides an independent validation of the role of correlations and MEC in enhancing the $1p1h$ transverse response in electron scattering.

The formalism developed here can be directly extended to quasielastic neutrino-nucleus scattering. In the Fermi gas, meson-exchange currents also produce a reduction of the $1p1h$ response, as in the electromagnetic case [20]. The main difference is that the weak response receives contributions from both vector and axial currents, in the one-body (OB) and two-body (MEC) sectors. Schematically, the modification of the matrix elements can be written as

$$\langle ph^{-1}|J^{\mu}_{\rm weak}|F\rangle = \langle p|J^{\mu}_{1b,V} + J^{\mu}_{1b,A}|h\rangle + \sum_{k<k_F} \langle pk|J^{\mu}_{2b,V} + J^{\mu}_{2b,A}|\phi_{hk} - \phi_{kh}\rangle,$$

where V and A denote vector and axial contributions, respectively, and the correlated wave functions ϕ_{hk} are obtained from the Bethe-Goldstone equation as before. Preliminary calculations indicate that the enhancement observed in the transverse electron response persists when the axial current is included, although a detailed study is required to quantify the effect. These results will be presented in a forthcoming publication.

5 Conclusions

We have developed a correlated model for the $1p1h$ transverse response including MEC and SRC within the independent pair approximation. Solving the Bethe-Goldstone equation with the Granada 2013 NN potential, we find that high-momentum components generate an enhancement that compensates the reduction predicted by the Fermi gas and reproduces the experimental data. The effect arises from coupled-channel waves, notably ${}^3S_1$–${}^3D_1$, highlighting the tensor force, and emerges directly from the realistic NN interaction without fitting. Our results are consistent with CBF calculations and suggest that a similar enhancement may occur in neutrino scattering.

Acknowledgements

The work was supported by Grant No. PID2023-147072NB-I00 funded by MICIU/AEI /10.13039/501100011033 and by ERDF/EU; by Grant No. FQM-225 funded by Junta de Andalucia.

References

[1] J. Jourdan, *Nucl. Phys.* **A** 603 (1996) 117.

[2] A. Bodek, M.E. Christy, *Phys. Rev. C* **106** (2022) L061305.

[3] J.E. Amaro, A.M. Lallena, G. Co, *Nucl. Phys. A* **578** (1994) 365-396.

[4] J. Carlson, J. Jourdan, R. Schiavilla, I. Sick, *Phys. Rev. C* **65** (2002) 024002.

[5] A. Lovato, S. Gandolfi, J. Carlson, S.C. Pieper, R. Schiavilla, *Phys. Rev. Lett.* **117** (2016) 082501.

[6] M. Kohno, N. Ohtsuka, *Phys. Lett. B* **98** (1981) 335-339.

[7] W.M. Alberico, T.W. Donnelly, A. Molinari, *Nucl. Phys. A* **512** (1990) 541.

[8] J.E. Amaro, A.M. Lallena, G. Co, *Int. J. Mod. Phys. E* **3** (1994) 735.

[9] J.E. Amaro, M.B. Barbaro, J.A. Caballero, T.W. Donnelly, A. Molinari, *Nucl. Phys. A* **723** (2003) 181-204.

[10] P.R. Casale, J.E. Amaro, M.B. Barbaro, *Symmetry* **15** (2023) 1709.

[11] P.R. Casale, J.E. Amaro, V. Belocchi, M.B. Barbaro, A. De Pace, M. Martini, *Phys. Rev. C* **112** (2025) 024603.

[12] A. Fabrocini, *Phys. Rev. C* **55** (1997) 338-348.

[13] P.R. Casale, J.E. Amaro, E.R. Arriola, I.R. Simo, *Phys. Rev. C* **108** (2023) 054001.

[14] H.A. Bethe, J. Goldstone, *Proc. Roy. Soc. (London)* **A238** (1957) 551.

[15] J. Goldstone, *Proc. Roy. Soc. (London)* **A239** (1957) 267.

[16] R. Navarro Pérez, J.E. Amaro, E. Ruiz Arriola, *Phys. Rev. C* **88** (2013) 064002; [erratum: *Phys. Rev. C* **91** (2015) 029901].

[17] D.O. Riska, *Phys. Rep.* **181** (1989) 207.

[18] R. Schiavilla, V.R. Pandharipande, D.O. Riska, *Phys. Rev. C* **40** (1989) 2294.

[19] P.R. Casale, J.E. Amaro, V.L. Martinez-Consentino, I.R. Simo, *Universe* **9** (2023) 158.

[20] P.R. Casale, J.E. Amaro, V. Belocchi, M.B. Barbaro, M. Martini, [arXiv:2507.20246 [hep-ph]].